2021 43rd Annual International Conference of the
IEEE Engineering in Medicine & Biology Society (EMBC)
Oct 31 - Nov 4, 2021. Virtual Conference

Quantifying the kinematic features of dexterous finger movements in nonhuman primates with markerless tracking

Ryan North, Rachele Wurr, Ryan Macon, Christopher Mannion, John Hyde, Abel Torres-Espin, Ephron S. Rosenzweig, Adam R. Ferguson, Mark H. Tuszynski, Michael S. Beattie, Jacqueline C. Bresnahan and Wilsaan M. Joiner, *Member, IEEE*

Abstract— **Research using nonhuman primate models for human disease frequently requires behavioral observational techniques to quantify functional outcomes. The ability to assess reaching and grasping patterns is of particular interest in clinical conditions that affect the motor system (e.g., spinal cord injury, SCI). Here we explored the use of DeepLabCut, an open-source deep learning toolset, in combination with a standard behavioral task (Brinkman Board) to quantify nonhuman primate performance in precision grasping. We examined one male rhesus macaque (*Macaca mulatta*) in the task which involved retrieving rewards from variously-oriented shallow wells. Simultaneous recordings were made using GoPro Hero7 Black cameras (resolution 1920 x 1080 at 120 fps) from two different angles (from the side and top of the hand motion). The task/device design necessitates use of the right hand to complete the task. Two neural networks (corresponding to the top and side view cameras) were trained using 400 manually annotated images, tracking 19 unique landmarks each. Based on previous reports, this produced sufficient tracking (Side: trained pixel error of 2.15, test pixel error of 11.25; Top: trained pixel error of 2.06, test pixel error of 30.31) so that landmarks could be tracked on the remaining frames. Landmarks included in the tracking were the spatial location of the knuckles and the fingernails of each digit, and three different behavioral measures were quantified for assessment of hand movement (finger separation, middle digit extension and preshaping distance). Together, our preliminary results suggest that this markerless approach is a possible method to examine specific kinematic features of dexterous function.**

Clinical Relevance— **The methodology presented below allows for the markerless tracking of kinematic features of dexterous finger movement by non-human primates. This method could allow for direct comparisons between human patients and non-human primate models of clinical conditions (e.g., spinal cord injury). This would provide objective quantitative metrics and crucial information for assessing movement impairments across populations and the potential translation of treatments, interventions and their outcomes.**

I. Introduction

Behavioral assessments of motor function in animal models of disease have ranged from observational rating scales (e.g., Basso, Beattie, Bresnahan, BBB Locomotor Rating Scale [1]), to simple measures on set tasks (e.g., time required for reward retrievals [2], [3]) to 3D kinematic metrics requiring advanced equipment and analytical techniques [4], [5]. Similarly, for human clinical diagnosis, qualitative scales such as the Jebsen-Taylor Hand function test or the GRASSP test [6], [7] have been used to simulate activities of daily living for patients [8]. While scales are powerful benchmarking tools and provide standardization across experiments and studies, they don't provide quantitative measures of movement kinematics (e.g., changes in position or velocity).

To obtain kinematic information, one common approach is to place physical markers at specific anatomical locations on animals to focus on joint movement. For example, Courtine et al. used reflective markers at bony landmarks in rats [4] to obtain the walking pattern of the animals before and after injury. In non-human primates, physical markers in conjunction with motion capture systems have been used to quantitatively examine reaching and grasping behavior [5], [9]. This type of quantitative data collection has provided more information on the detailed motor behavior while still concurrently obtaining simpler measures of task performance such as success rate, time to completion, etc. However, these types of marker-based tracking methods can affect the natural behavior of the animal and consequently affect the behavioral analysis [10].

Recently, more advanced computational techniques such as DeepLabCut allow for the tracking of anatomical locations without the use of physical markers during movement [11]. Previous uses of DeepLabCut include reach and grasp tasks for mice (3D information) and more naturalistic studies conducted on non-human primates (2D information) [9]–[15]. In both animal models, DeepLabCut was able to achieve sufficient tracking so that further quantitative analysis could be performed. That is, the specific landmarks were accurately tracked (e.g., the individual digits in the rat model) allowing further analyses of movement kinematics.

Here we present a methodology which will allow for the recording and analysis of behavioral data when a monkey is completing the Brinkman board task (as presented in [19] and described in D of the Methodology below) using DeepLabCut [20]. Although preliminary, this study demonstrates the feasibility of extracting quantitative kinematic movement information (e.g., finger extension), based on the anatomical features of the digits, without the use of physical markers. This would be an advancement over previous techniques in that natural grasping behavior is minimally influenced.

II. Methodology

A. Animal

In this study, one rhesus macque (*Maca mulatta*, male age 7 years 11 months, weight of 11.70kg) was used. This animal

was housed at the California National Primate Research Center, Davis, CA; all primate procedures were approved by the California National Primate Research Center Institutional Animal Care and Use Committee.

B. Behavioral Setup Design

We modified a previous setup that requires bimanual movements to retrieve food rewards from the Brinkman board [19]. The left hand must depress the lever through the left porthole to allow the right hand to interact with the Brinkman board and retrieve the food reward. Figure 1 shows a front view of the apparatus while the animal performs the task. The locations of the cameras were chosen to ensure that they can capture the full view of the animal's right hand completing the task, but are inaccessible to the animal. The side camera was placed 10.8 cm away from the closest side of the Brinkman board tray and sat in a small housing to ensure that it can be easily removed and placed again in the same location. The camera is surrounded by three Plexiglas walls with an opening that is only accessible to the trainer/tester and not the animal. The top camera was placed 28.6 cm away from the surface of the Brinkman board and was centered on the board. A small housing was created around the top camera so that it was also inaccessible to the animal. Additionally, both housings for the cameras stabilized the camera during testing, countering any device motion due to the animal.

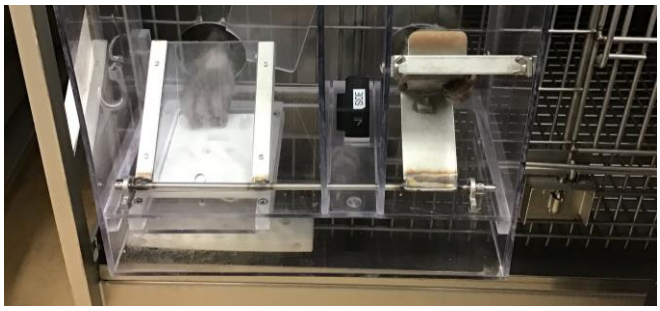

Figure 1. *Animal performing the Brinkman board task using the behavioral setup. The lever must be pushed by the left hand in order for the right hand to have access to the Brinkman board. Cameras were placed above and to the right of the animal's hand, both of which were inaccessible to the animal.*

C. Camera Selection

The GoPro Hero 7 Black was selected based on several criteria as summarized by Table I.

TABLE I. CAMERA SELECTION CRITERION

Characteristic	***Desired***
Camera size	<120 cm^3
Camera weight	<200 g
Recording resolution	>1080p
Frame rate	≥90 frames per second
External SD card support	>128gb
Standard video format	.mp4
Video stability assist	
Replaceable battery	
Shock resistance	
Water resistance/proof	
Mounting hardware support	
Product support	

These characteristics allowed for minimal changes to the existing behavioral setup, while allowing for future quantitative analysis. For example, the camera size was a strong factor when deciding camera type, as the overall size and dimensions of the behavioral setup could not be changed and the camera must be removable.

D. Behavioral Hand Task (The Brinkman Board Task)

The animal was trained to use his right hand to retrieve food rewards from the wells on the Brinkman board. These rewards varied to optimize the motivation of the animal (e.g. yogurt covered raisins, nuts, etc.) but maintain a consistent reward size. Performance on the board is typically assessed by a numerical score (between 0-3) based on the animal's ability to pinch, retrieve food rewards without dropping it and transfer that reward to their mouth. The animal was given 60 seconds to clear each board. In the preliminary analysis described here, eight unique Brinkman boards were presented, which constitutes one session. The animal then completed two more sessions within the same day to allow for more videos to be included in the DeepLabCut analysis (described in section F). These Brinkman boards varied in the number of wells (1-9) and the well orientation. Examples of these Brinkman boards are shown below in Figure 2.

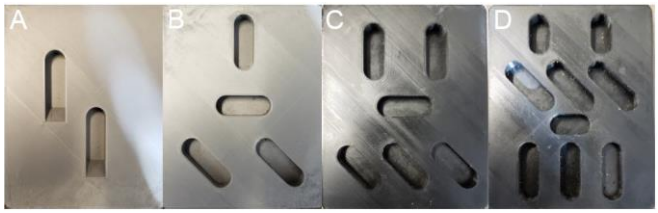

Figure 2. *Depiction of four example Brinkman boards. Note the differences in the number of reward wells (2, 4, 7 and 9) and orientation with respect to hand movement (45°,90°, and 180°).*

E. Video Collection

Recording of the task begins when the Brinkman board is presented to the animal and ends when the animal either successfully removes all the rewards from the Brinkman board or reaches the 60 second timeout period. This process is repeated until the animal completes the total number of Brinkman boards (8) for a given session. These videos are recorded at a resolution of 1920 x 1080 pixels at 120 frames per second in an mp4 format. These videos are then imported into DeepLabCut for further analysis.

F. DeepLabCut Analysis

DeepLabCut is a deep learning toolset that allows for the markerless tracking of various locations across multiple video frames [11]. In this specific case, two networks were trained corresponding to the two cameras (Top and Side) using 400 manually annotated images from 16 different videos (25 images from each video determined by a k-means algorithm for visual uniqueness) from 2 separate sessions of the Brinkman board task. In these annotated images, the following landmarks in the videos of the right hand were of interest (locations of fingertips and knuckles of the five digits) as summarized in Table II. Examples of the side and top view camera frames, with the color coded markers of the landmarks, are shown in Figure 3A and B, respectively.

TABLE II. FEATURES OF INTEREST

Feature	***Locations***
Thumb Digit (D1)	Fingertip, 1st Knuckle and 2nd Knuckle
Index Digit (D2)	Fingertip, 1st Knuckle, 2nd Knuckle, and 3rd Knuckle
Middle Digit (D3)	Fingertip, 1st Knuckle, 2nd Knuckle, and 3rd Knuckle
Ring Digit (D4)	Fingertip, 1st Knuckle, 2nd Knuckle, and 3rd Knuckle
Pinky Digit (D5)	Fingertip, 1st Knuckle, 2nd Knuckle, and 3rd Knuckle

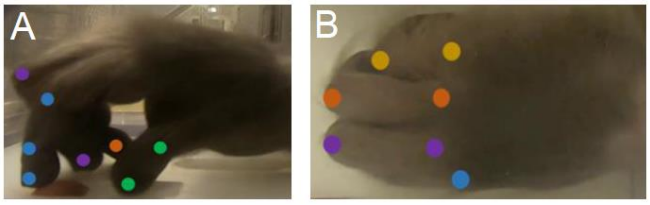

Figure 3. (A) *Side view of marked locations. Only the index and thumb digits are fully markered. The remaining locations are occluded from this camera angle. For example, the 1st knuckle of the middle digit (D3) is occluded by the index digit (D2).* ***(B)*** *Top view of markered locations at a different timepoint with respect to panel A. The top view mainly focuses on the 2nd and 3rd knuckle locations of all the digits. Similar to panel A, not all locations are markered as they are occluded by other digits. Specifically, the 2nd knuckle of the index digit (D2) is folded under (occluded) the middle digit (D3).*

Following the recommend procedure [11], this method yielded a side camera trained pixel error of 2.15 (this represents the root mean square error between user and DeepLabCut values using images the DeepLabCut neural network were trained on), test pixel error of 11.25 (which represents a max error of 1.04%. This error is the root mean square error between user and DeepLabCut using images naive to the DeepLabCut neural network training); top camera trained pixel error of 2.06, test pixel error of 30.31 (which is a max error of 2.81%). These values were comparable to a previous primate study, and thus were judged sufficient for additional tracking on the remaining videos [15]. The comma-separated values (CSV) file output from DeepLabCut was then imported into MATLAB for further analysis.

G. Filtering

The CSV file was imported into MATLAB where the data were filtered by the confidence value given by DeepLabCut at each time point. A confidence threshold of 0.8 was set. This value was determined as the balance of having enough accurate points as determined by DeepLabCut and by visually validating the locations of those markers. If the value fell below the threshold, it was replaced with an average of the 12 values surrounding it. The data were further filtered by a box filter with a size of 30 data points to smooth out the movements. Lastly, the values were converted from pixel space to cm using a basic linear conversion based on the dimensions of the Brinkman board.

H. Quantitative Behavioral Analysis

Based on the filtered kinematic data, the following parameters were quantified. These were chosen based on movement features often examined in the human patients and previous non-human primate studies, such as those examining precision grasp [21]–[23]. Finger extension and finger separation were determined using the top camera view, and hand preshaping was determined using the side camera view.

Finger Extension

Finger extension was determined as the Euclidean distance between the 2nd knuckle and the 3rd knuckle within a digit. The 2nd knuckle was chosen over the 1st knuckle or fingertip as it was consistently in view/frame and its tracking was more stable across sessions. Figure 4 shows this measure, represented by the white bidirectional arrow.

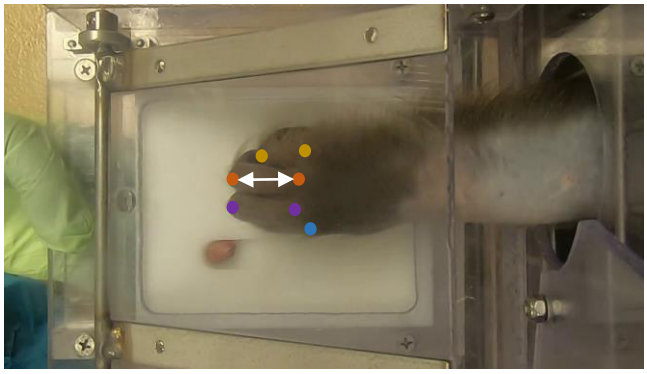

Figure 4. *Depiction of finger extension. Each filled circle represents the location tracked in the video (e.g., filled purple circles represent the knuckles of the middle digit, D3). The double white arrow is the finger extension of 3.61 cm between the 2nd and 3rd knuckle of the ring digit (D4).*

Finger Separation

Finger Separation was defined as the Euclidean distance between digits at the 2nd knuckle. The 2nd knuckle was selected due to it being consistently in view/frame. Figure 5 shows this measure, as represented by the white bidirectional arrow.

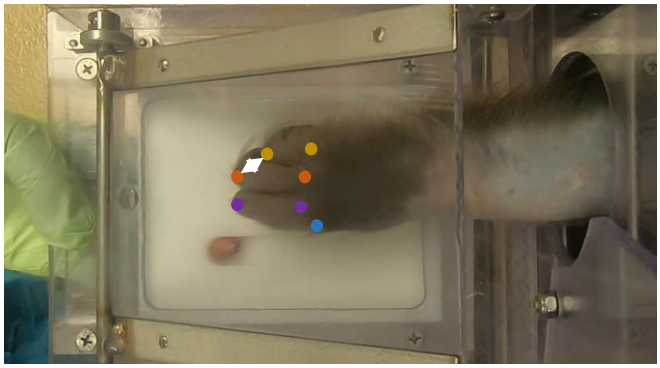

Figure 5. *Depiction of finger separation. As in Figure 4 each filled circle represents the location tracked in the video (e.g., filled purple circles represent the knuckles of the middle digit, D3). The double white arrow is the finger separation of 0.77 cm between the 2nd knuckles of the ring and pinky (D4 and D5) digits.*

Hand Preshaping

Hand preshaping was defined as the Euclidean distance between the thumb (D1) fingertip/fingernail and the index (D2) fingertip/fingernail. Figure 6 shows the distance between these locations during the Brinkman board task as the animal attempts to retrieve the food reward.

Figure 6. *Depiction of hand preshaping. As in Figures 4 and 5 each filled circle represents the location tracked in the video (e.g., filled green circles represent the knuckles of the thumb digit, D1). The double white arrow is the finger separation between the tip of the index (D2) and thumb (D1), 1.25 cm in this example.*

III. Results

In all cases described below, the animal successfully retrieved all the food rewards from the Brinkman boards under the 60 second threshold for timeout.

Finger Extension

Figures 7A and B show differences in finger extension between two different Brinkman boards along with the maximum value determined within the same testing session. The different oriented wells required changes in the hand angle and thus, different amounts of finger extensions. For performance on the two different boards, we determined the time of max finger extension when retrieving the rewards. Figure 7A is performance on Brinkman board A in Figure 2 and has a maximum finger extension of 3.71 cm. Figure 7B is performance on Brinkman board C in Figure 2 and the animal has a maximum finger extension of 4.81 cm.

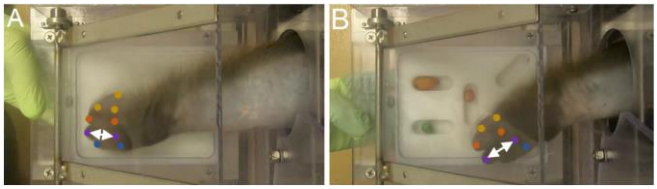

Figure 7. (A) *Finger extension on Brinkman board A (Figure 2A). In this example, the animal had a maximum finger extension of 3.71 cm.* ***(B)*** *Finger extension on Brinkman board C (Figure 2C). In this example, the animal had a maximum finger extension of 4.81 cm.*

Finger Separation

Similar to Figure 7, Figures 8A and B show the difference of finger separation when the animal is completing the Brinkman board task. As for finger extension, the different oriented wells required different amounts of finger separation. For performance on two different boards, we determined the time of max finger separation when retrieving the rewards. Figure 8A is performance on Brinkman board A in Figure 2

and has a maximum finger separation of 1.39 cm. Figure 8B is performance on Brinkman board D in Figure 2 and the animal has a maximum finger separation of 2.53 cm.

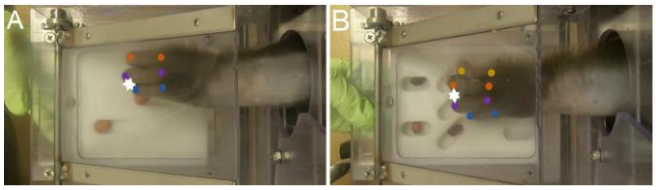

Figure 8. (A) *Finger separation on Brinkman board A. In this case, the animal had a maximum finger separation of 1.39 cm.* ***(B)*** *Finger separation on Brinkman board D. In this case, the animal had a maximum finger separation of 2.53 cm.*

Hand Preshaping

An example of preshaping for one reach/grasp on Brinkman board A (Figure 2) is shown in Figure 9. The change in the distance between the thumb (D1) and the index (D2) fingertip during the retrieval motion is shown in Figure 10. As shown in the plot, the distance starts at 3.5 cm and then decreases to 1.25 cm at food retrieval. The labels A, B and C on the plot in Figure 10 correspond to the video frames shown in Figures 9A, B and C, respectively.

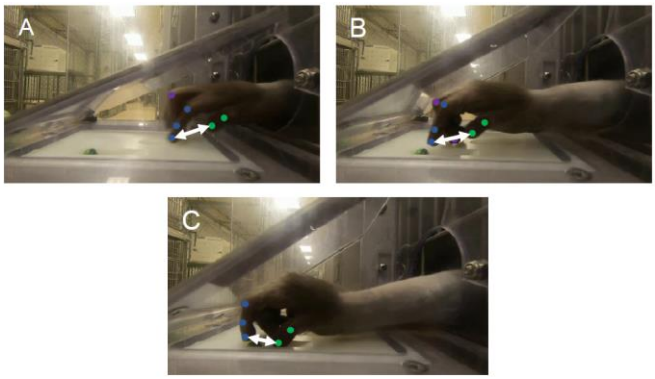

Figure 9. (A) *Video frame of timepoint A in Figure 10, an approximate distance of 3.5 cm between the index digit and thumb (D2 and D1).* ***(B)*** *Video frame of timepoint B in Figure 10, an approximate distance of 3.0 cm between the index and thumb digit, which is a slight decrease from timepoint A.* ***(C)*** *Video frame of timepoint C in Figure 10, an approximate distance of 1.25 cm between the index and thumb digit. At this point, the animal has nearly competed the reaching motion to the food reward.*

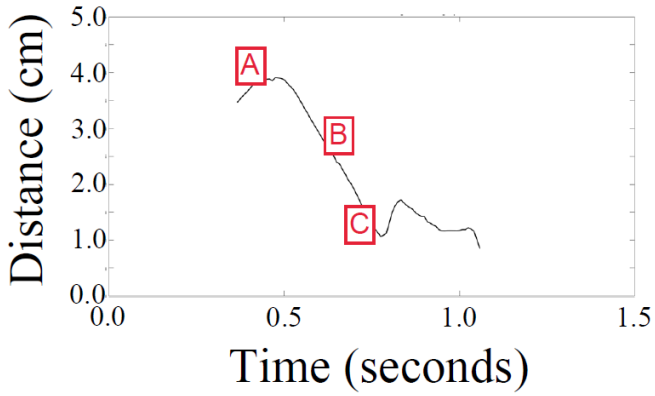

Figure 10. Plot of preshaping (distance between the index digit and thumb, D2 and D1) during food retrieval over time for one reach/grasp on Brinkman board A (Figure 2). Labels A, B and C correspond to the frames in Figure 9.

IV. Conclusion and Future Work

Here we present a methodology which allows for the markerless tracking of different anatomical features during dexterous finger movements in nonhuman primates. Specifically, we show that a two camera setup combined with the DeepLabCut algorithm can quantify several features of finger movements (separation, extension and preshaping) while nonhuman primates retrieve food rewards from differently oriented wells. This approach could compliment current qualitative scales used for behavioral assessments by providing quantitative kinematic measures of motor behavior. In our future work we will apply this analysis over the time frames of recovery for different animal models (e.g., spinal cord injury) and determine the extent these measures relate to other metrics of successful reaches/grasps (e.g., success rate, time to complete tasks, etc.). Additionally, we will examine the variance of these measures across trials and sessions to quantify performance consistency—a key element of stereotypical motor behavior. Importantly, this methodology may provide a means to rigorously quantify the extent to which dexterous motor behaviors reflect the abilities preceding injury and provide measures that are sensitive to the injury and treatments. If successful, this would provide critical information to evaluate the functional effectiveness of novel interventions for clinical conditions that affect the motor system.

Acknowledgments

Veterans Administration (IP50RX001045 RR&D B7332R; RR&D 1I01RX002245)
NIH (NS104442; NS105478; NCRR P51 OD011107)
DoD CDMRP (SC170233)
DARPA (N660012024046)
Dr. Miriam and Sheldon G. Adelson Medical Research Foundation

Craig H. Neilsen Foundation
Bernard and Anne Spitzer Charitable Trust

REFERENCES

[1] D. M. Basso, M. S. Beattie, and J. C. Bresnahan, "A Sensitive and Reliable Locomotor Rating Scale for Open Field Testing in Rats," *J. Neurotrauma*, vol. 12, no. 1, pp. 1–21, Feb. 1995, doi: 10.1089/neu.1995.12.1.

[2] H. Klüver, "An Auto-Multi-Stimulation Reaction Board for Use with Sub-Human Primates," *J. Psychol.*, vol. 1, no. 1, pp. 123–127, Jan. 1935, doi: 10.1080/00223980.1935.9917246.

[3] E. Schmidlin *et al.*, "Behavioral Assessment of Manual Dexterity in Non-Human Primates," *J. Vis. Exp.*, no. 57, p. 3258, Nov. 2011, doi: 10.3791/3258.

[4] G. Courtine *et al.*, "Recovery of supraspinal control of stepping via indirect propriospinal relay connections after spinal cord injury," *Nat. Med.*, vol. 14, no. 1, Art. no. 1, Jan. 2008, doi: 10.1038/nm1682.

[5] L. Friedli *et al.*, "Pronounced species divergence in corticospinal tract reorganization and functional recovery after lateralized spinal cord injury favors primates," *Sci. Transl. Med.*, vol. 7, no. 302, p. 302ra134, Aug. 2015, doi: 10.1126/scitranslmed.aac5811.

[6] S. Kalsi-Ryan, A. Curt, M. Fehlings, and M. Verrier, "Assessment of the Hand in Tetraplegia Using the Graded Redefined Assessment of Strength, Sensibility and Prehension (GRASSP): Impairment Versus Function," *Top. Spinal Cord Inj. Rehabil.*, vol. 14, no. 4, pp. 34–46, Apr. 2009, doi: 10.1310/sci1404-34.

[7] S. Kalsi-Ryan, A. Curt, M. C. Verrier, and M. G. Fehlings, "Development of the Graded Redefined Assessment of Strength, Sensibility and Prehension (GRASSP): reviewing measurement specific to the upper limb in tetraplegia," *J. Neurosurg. Spine*, vol. 17, no. 1 Suppl, pp. 65–76, Sep. 2012, doi: 10.3171/2012.6.AOSPINE1258.

[8] R. H. Jebsen, N. Taylor, R. B. Trieschmann, M. J. Trotter, and L. A. Howard, "An objective and standardized test of hand function," *Arch. Phys. Med. Rehabil.*, vol. 50, no. 6, pp. 311–319, Jun. 1969.

[9] J. Zhuang, W. Truccolo, C. Vargas-Irwin, and J. P. Donoghue, "Decoding 3-D Reach and Grasp Kinematics From High-Frequency Local Field Potentials in Primate Primary Motor Cortex," *IEEE Trans. Biomed. Eng.*, vol. 57, no. 7, pp. 1774–1784, Jul. 2010, doi: 10.1109/TBME.2010.2047015.

[10] A. Nakamura *et al.*, "Low-cost three-dimensional gait analysis system for mice with an infrared depth sensor," *Neurosci. Res.*, vol. 100, pp. 55–62, Nov. 2015, doi: 10.1016/j.neures.2015.06.006.

[11] A. Mathis *et al.*, "DeepLabCut: markerless pose estimation of user-defined body parts with deep learning," *Nat. Neurosci.*, vol. 21, no. 9, pp. 1281–1289, Sep. 2018, doi: 10.1038/s41593-018-0209-y.

[12] L. Ruder, R. Schina, H. Kanodia, S. Valencia-Garcia, C. Pivetta, and S. Arber, "A functional map for diverse forelimb actions within brainstem circuitry," *Nature*, vol. 590, no. 7846, Art. no. 7846, Feb. 2021, doi: 10.1038/s41586-020-03080-z.

[13] R. Storchi *et al.*, "A High-Dimensional Quantification of Mouse Defensive Behaviors Reveals Enhanced Diversity and Stimulus Specificity," *Curr. Biol.*, vol. 30, no. 23, pp. 4619-4630.e5, Dec. 2020, doi: 10.1016/j.cub.2020.09.007.

[14] A. Bova, K. Kernodle, K. Mulligan, and D. Leventhal, "Automated Rat Single-Pellet Reaching with 3-Dimensional Reconstruction of Paw and Digit Trajectories," *J. Vis. Exp. JoVE*, no. 149, Jul. 2019, doi: 10.3791/59979.

[15] J. M. Barrett, M. G. R. Tapies, and G. M. G. Shepherd, "Manual dexterity of mice during food-handling involves the thumb and a set of fast basic movements," *PLOS ONE*, vol. 15, no. 1, p. e0226774, Jan. 2020, doi: 10.1371/journal.pone.0226774.

[16] B. J. Forys, D. Xiao, P. Gupta, and T. H. Murphy, "Real-Time Selective Markerless Tracking of Forepaws of Head Fixed Mice Using Deep Neural Networks," *eNeuro*, vol. 7, no. 3, Jun. 2020, doi: 10.1523/ENEURO.0096-20.2020.

[17] K. Sehara, P. Zimmer-Harwood, M. E. Larkum, and R. N. S. Sachdev, "Real-time closed-loop feedback in behavioral time scales using DeepLabCut," *eNeuro*, Feb. 2021, doi: 10.1523/ENEURO.0415-20.2021.

[18] R. Labuguen, D. K. Bardeloza, S. B. Negrete, J. Matsumoto, K. Inoue, and T. Shibata, "Primate Markerless Pose Estimation and Movement Analysis Using DeepLabCut," in *2019 Joint 8th International Conference on Informatics, Electronics Vision (ICIEV) and 2019 3rd International Conference on Imaging, Vision Pattern Recognition (icIVPR)*, May 2019, pp. 297–300, doi: 10.1109/ICIEV.2019.8858533.

[19] E. S. Rosenzweig *et al.*, "Chondroitinase improves anatomical and functional outcomes after primate spinal cord injury," *Nat. Neurosci.*, vol. 22, no. 8, Art. no. 8, Aug. 2019, doi: 10.1038/s41593-019-0424-1.

[20] Y. S. Nout *et al.*, "Methods for Functional Assessment After C7 Spinal Cord Hemisection in the Rhesus Monkey," *Neurorehabil. Neural Repair*, vol. 26, no. 6, pp. 556–569, Jul. 2012, doi: 10.1177/1545968311421934.

[21] M. Santello, M. Flanders, and J. F. Soechting, "Patterns of Hand Motion during Grasping and the Influence of Sensory Guidance," *J. Neurosci.*, vol. 22, no. 4, pp. 1426–1435, Feb. 2002, doi: 10.1523/JNEUROSCI.22-04-01426.2002.

[22] S. A. Winges, D. J. Weber, and M. Santello, "The role of vision on hand preshaping during reach to grasp," *Exp. Brain Res.*, vol. 152, no. 4, pp. 489–498, Oct. 2003, doi: 10.1007/s00221-003-1571-9.

[23] N. B. W. Macfarlane and M. S. A. Graziano, "Diversity of grip in Macaca mulatta," *Exp. Brain Res.*, vol. 197, no. 3, pp. 255–268, Aug. 2009, doi: 10.1007/s00221-009-1909-z.